Heliyon 10 (2024) e26329

Contents lists available at ScienceDirect

Heliyon

journal homepage: www.cell.com/heliyon

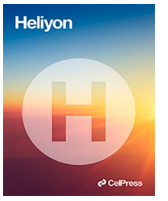

Research article

Mode I fracture analysis of aluminum-copper bimetal composite using finite element method

Vahid Yousefi Mehr, Mohammad Reza Toroghinejad *

Isfahan University of Technology, Department of Materials Engineering, Isfahan University of Technology, Isfahan, 84156-83111, Iran

ARTICLE INFO

Keywords:
Fracture analysis
Al–Cu bimetal
Simulation
Roll bonding
Experiment

ABSTRACT

The properties of Al–Cu bimetallic composite are investigated employing the finite element method to understand the nature of the composite materials under different loading conditions. In this regard, Al and Cu metallic sheets were implemented to analyze cold-roll bonding (CRB) and to monitor the bonding conditions. After rolling the materials were investigated for their stress distribution and bonding as well as fracture behavior. Finite element investigation was used by the ANSYS software to analyze the stress-strain distribution in the metal layers. The results indicate that the appropriate joining of Al–Al and Al–Cu can be achieved using the CRB process. The stress distribution based on the Von-Mises criterion was calculated and validated by simulation studies. For crack simulations, on the other hand, the results showed that during crack propagation, the materials showed different behaviors owing to the varying properties of Al and Cu. Also, for both the tests, stress distribution in 2D and 3D were simulated, and different stress criteria were obtained and compared. Moreover, optical and scanning electron microscopies were used to study the characteristics of the materials and to support FEM outputs.

1. Introduction

Multi-metallic materials are promising for practical applications and economic purposes, thus gaining notable attention in recent decades [1–6]. There are several ways to produce composite materials such as casting [7], however, the roll bonding (RB)-based method is a simple and cheap way to manufacture such materials [8–12]. Among numerous experimental exercises for producing similar [13–17] and dissimilar [18–26] metal-metal composites, Al and Cu were interesting due to their similar crystal structure and their ability to deform in different shapes [27–30]. For this purpose, the researchers including the present authors decided to evaluate and produce Al–Cu composites and evaluate their properties using different methods [28,31,32]. In one study, a variety of processing parameters were evaluated that affected the metal bonding condition only experimentally [33]. However, recent attention to materials simulations motivated the authors to model the behavior of this material using the finite element method (FEM). This method is widely accepted for different mechanical applications [34]. Also, the roughness of the metal surface contributes to the roll bonding process [35]. It is also stated that parameters such as crystal structure, grain size, and strain are key factors in determining bonding [35]. In a study [36], a group of researchers evaluated the bonding of AA 1050/AA 6061 and analyzed the interface of the material using experimental and simulation studies. In the research, the rolling speed was optimized to develop an appropriate condition for bonding. Other researchers [37] evaluate the characteristics of Cu/Ti composite by the accumulative roll bonding (ARB) process. They modeled

* Corresponding author.
E-mail addresses: v.yousefi@alumni.iut.ac.ir (V. Yousefi Mehr), toroghi@iut.ac.ir (M.R. Toroghinejad).

https://doi.org/10.1016/j.heliyon.2024.e26329
Received 15 November 2023; Received in revised form 5 February 2024; Accepted 12 February 2024
Available online 13 February 2024
2405-8440/Â© 2024 The Authors. Published by Elsevier Ltd. This is an open access article under the CC BY-NC-ND license (http://creativecommons.org/licenses/by-nc-nd/4.0/).

shear banding and layer thickness during deformation using FEM successfully. Also, a group of scientists [38] investigated the Cu/Ti composite properties using analytical and experimental methods. It is claimed that a harder layer can respond to the rolling pressure by fracturing. Besides, a model based on fluctuaion wavelength was used to support the evidence. Also, it is stated that a FEM can be successfully used to validate the pile-up data obtained from experimental results for ARBed Cu/Nb nanolaminates [3]. For fracture toughness, on the other hand, a group of researchers stated that by increasing the number of roll bonding cycles of an Al5052–Cu composite, Kc showed a considerable increase [30].

The FEM, therefore, is an easier and cheaper tool for engineers to access and evaluate data obtained by experiments. The need for materials modeling through the FEM as well as complementing our previous studies is the motivation of the present investigation. The authors, proposed an experimental procedure for manufacturing the Al–Cu material followed by simulations of materials under loading and strain-stress distribution using ANSYS software. Also, a hypothesis crack is proposed to evaluate the deformation around the tip of the crack for both individual layers (Al and Cu). Moreover, microstructural studies using microscopy techniques were used to support the FEM results. Thus, this study aims to investigate the details affecting Al–Cu material characteristics and support the experimental studies.

2. Material selection and FEM analyses

The cold roll bonding process is used to simulate the joining the metals with non-linear behavior i.e., Al and Cu alloys. Materials' initial characteristic is summarized in Table 1. The Al and Cu layers (10 cm × 2.5 cm × 0.5 mm), were first designed based on the experiment which was cut from the initial sheet. The metals were then rolled with a rolling mill machine of 20 tons capacity for a specific reduction in thickness (a schematic illustration of the CRB process is shown in Fig. 1). The friction coefficient of the rollers and the surface of the sample is evaluated to be 0.1. The speed of the rolling process was kept at about 2 m/min to secure appropriate joining. The resulting composites were then simulated for the peeling test according to ASTM D1876-08 standard. After the mechanical tests, some samples were prepared for optical and scanning electron microscopies (OM and SEM) on rolling direction (RD)-transverse direction (TD), and normal direction (ND)-TD planes. The simulation studies were conducted using raw data from experimental input and implemented in ANSYS software such as bonding conditions and V-notched samples. All the rolling procedures stated above were simulated in two-dimension (2D) and three-dimension (3D) based on the laboratory's inputs and then the data were collected from simulation studies for validation and analysis. The experimental and simulation outputs were then used for investigation/comparison in this research. Furthermore, different symbols used in the study are tabulated in Table 2.

3. Results and discussion

3.1. CRB and peeling test

The most important step in manufacturing the Al–Cu composite is the possibility of bonding the Al and Cu layers through the rolling process. To evaluate this phenomenon quantitatively, a peeling test was used. The results indicated that the bonding is strong enough for desired applications based on provided parameters [33]. The deformation induced by the pressure of the rollers plays the main role in establishing an appropriate bonding. The authors first investigated [33] different parameters affecting the bonding condition including the reduction of the rollers, and the effect of an oxide film. However, some other issues remained unclear such as the effect of rolling conditions on the deformation and how rollers could provide deformation to result in a metal-metal bonding. For this purpose, the process was simulated and the boundary condition based on experimental information was utilized to study the materials' behavior. The results are interesting as shown in Fig. 2. At first, it is noted that the end part of the joints deviated in a specific direction as pointed by the arrows in Fig. 2 (a) and (b). One may argue that this deviation could be a software error. However, as we alternated the layers (Al on the top and Cu on the bottom), the deviation was again observed in a diverse direction. Also, two similar metals were examined similarly (Al–Al as seen in Fig. 2 (c)) to see if the same condition may be obtained. Surprisingly, the deviation diminished when a similar metal-metal was used. In practice, at the laboratory, a similar deviation was observed during the CRB process of two dissimilar metals. The deviation was not a FEM error but the reason underlying this phenomenon should be related to the metals' properties [39]. Generally, Al is a softer metal which means that during the rolling, it can be easily deformed as compared to the Cu layer (known as a harder metal). But, the harder layer, i.e., Cu, response to the rolling pressure was different as compared to the Al. This is because Cu cannot be shaped as easily as Al can. As a result, the composite deviated towards the harder (Cu) layer during the rolling process. In fact, in the rolling gap, the deformation that was responsible for the deviation of the metals was accommodated by the extension of the strips. This process, in turn, led to metal-to-metal bonding as discussed later. The stress distribution for this process is elaborated in the following paragraphs in detail.

Another observation in the CRB process that can be concluded from Fig. 2 is the way stress is distributed through the Al and Cu sides. In the cold rolling, the stress distribution on the Cu side is different during the CRB process as compared to that of other metals i.

Table 1
Characteristics of the initial materials.

	Young modulus (GPa)	Poisson ratio	Bulk modulus (GPa)	Density (kg.m^{-3})
Al	71	0.33	69	2770
Cu	110	0.34	114	8300

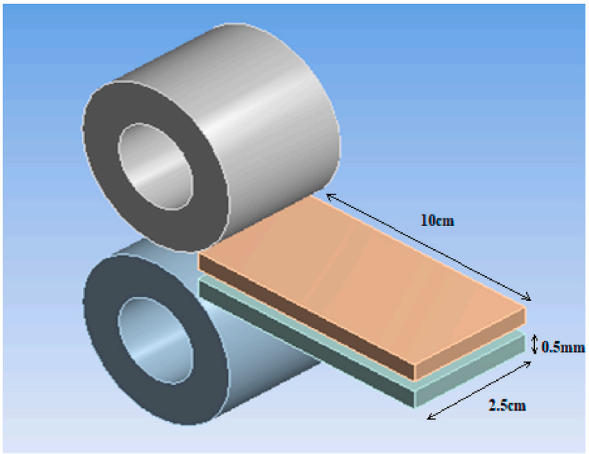

Fig. 1. A schematic illustration of the CRB process.

Table 2
Symbols used in this research.

K_I	P	σ	a	c	w	ρ
Stress intensity factor	Compressive rolling stress	Tension	Length of crack	Total thickness	Thickness of layer	The radius of the crack tip
R	**h**	**μ**	**ε**	**f (μ)**	**σ_{max}**	**σ_0**
The radius of the rollers	Ratio of sheet thickness	Friction coefficient	Strain	Geometric shape factor	Maximum tension in front of the crack	Flow stress

e., Al. The Al, in contrast, experiences different levels of deformation as highlighted by colored contours in this figure. Also, by comparing Fig. 2 (a) and (b) with CRBed Al–Al metals in Fig. 2 (c), one may conclude that the distribution of deformation is more uniform for Al–Al material. The main reason is that metals' behavior is varied during the deformation process. In fact, Al has a higher stacking fault energy (166 mJ/m^2) as compared to Cu (78 mJ/m^2) [39]. Therefore, the Al layer can be easily deformed because the movement of the dislocations is easier during the rolling process. Consequently, Al experienced less work hardening than Cu did. While the Cu layer can be work-hardened more efficiently, thus, deformation is varied in Cu and the rollers induced more stress on the Cu layer to shape it plastically during the rolling as indicated in Fig. 2 and as confirmed earlier.

Moreover, for a detailed perspective, a 3D model based on the experimental results was designed and the composite materials were obtained directly from ANSYS software to further support the abovementioned claims (Fig. 3, note that Al is the top layer). Also, the level of Von-Mises stress induced by the rollers was collected as seen in Fig. 4. As seen, for Al–Al the amounts of stress are lower as compared to that of Al–Cu. This means that when two soft metals are bonded, rollers provide a much lower amount of stress for shaping/joining the metals. However, in Al–Cu, the deformation becomes complicated because of the effect of two dissimilar metals. As such, the Al–Cu material experienced a higher level of stress which is due to the rollers' pressure as confirmed in Fig. 4.

To validate the numerical value in simulation in Fig. 3, the following elaborations are suggested. As seen in this figure, the Von-Mises stress showed a wide range between near 0 and 725 MPa. In the present condition, the following equations are useful to obtain stress distribution during the rolling process based on ref [40]:

$$\varepsilon_y = \frac{d\sigma}{d\varepsilon}\left(\sigma_y - \frac{1}{2}(\sigma_x + \sigma_z)\right) = 0 \tag{1}$$

We can assume that $\sigma_x = 0$, because the stress is zero in this direction, then from equation (1), it can be concluded that $\sigma_y = \frac{\sigma_z}{2}$. Also, it can be assumed that the stress of the roller (P) equals to σ_z (or $-\sigma_z = P$). Moreover, for the relation of shear stress, friction coefficient, and applied force, equation (2) can be used:

$$\tau_{zx} = \mu P = 0.1\,P \tag{2}$$

Also, a three-dimensional stress tensor as seen in the following matrix can be developed:

$$\sigma_{ij} = \begin{pmatrix} 0 & 0 & \tau_{xz} \\ 0 & -0.5\sigma_z & 0 \\ \tau_{xz} & 0 & -\sigma_z \end{pmatrix} = \begin{pmatrix} 0 & 0 & \mu p \\ 0 & 0.5p & 0 \\ \mu p & 0 & p \end{pmatrix} \tag{3}$$

where, based on equation (3) we can compute (I) by solving the matrix i.e., $I_1 = 1.5\,p$, $I_2 = -0.49\,p^2$, and $I_3 = -0.005\,p^3$. Then, the calculation should be continued to measure principal stresses, therefore, equations (4) and (5) must be used [40]:

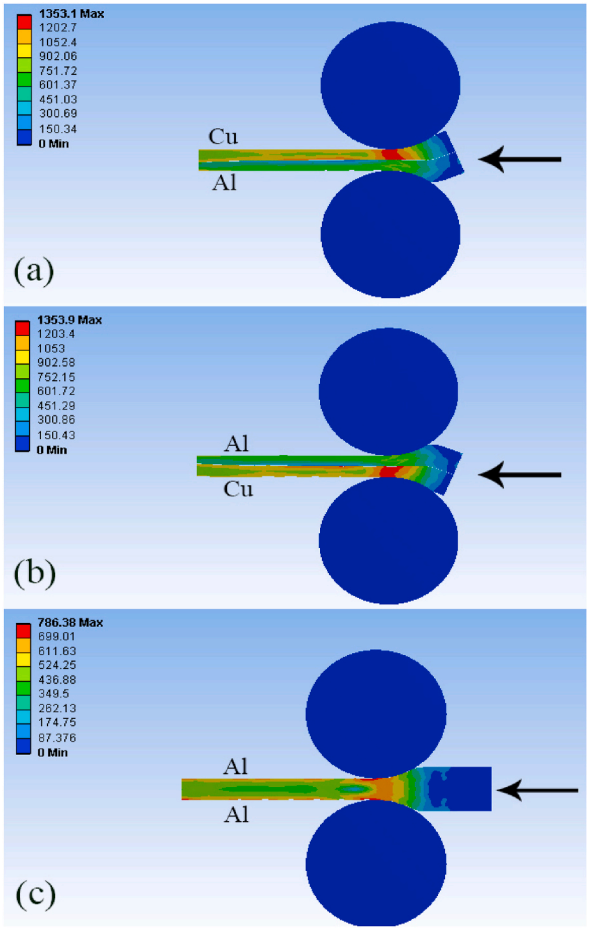

Fig. 2. A 2D simulation of the rolling process with different conditions, a) Cu is on the top, b) Al is on the top, and c) two Al layers were used simultaneously [note the end part of the layers which is indicated by the arrows].

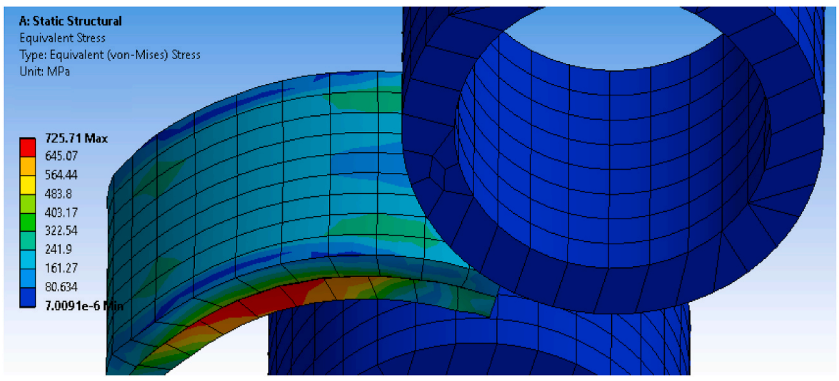

Fig. 3. A 3D simulation of the CRBed Al-Cu material with the corresponding Von-Mises stress distribution.

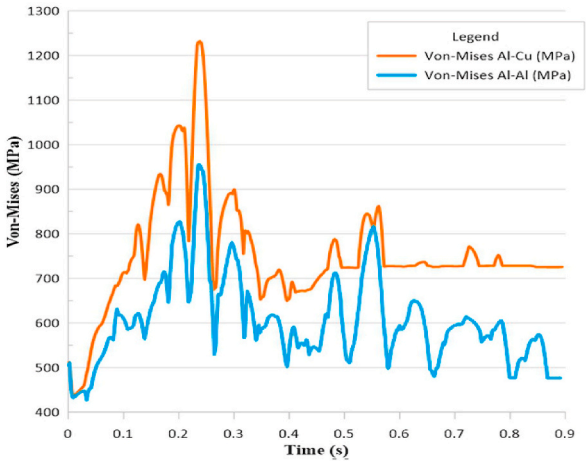

Fig. 4. Diagrams of Von-Mises stress variations that are induced by the rollers for Al–Al and Al–Cu CRBed materials.

$$p = \frac{h}{\mu L}\left(exp\left(\frac{\mu L}{h}\right) - 1\right)\sigma_0 \tag{4}$$

Where L is:

$$L = \sqrt{R\Delta h} \tag{5}$$

In these equations, σ_0 is flow stress (similar calculations were also used in Ref. [29]). Also, Δh is the average of the difference of initial and final thicknesses. Now, the compressive rolling stress i.e., $P = 530.5$ MPa can be obtained. Finally, the principal stresses are computed as follows:

$$\sigma^3 - I_1\sigma^2 - I_2\sigma - I_3 = 0 \tag{6}$$

Three principal stresses, therefore can be obtained by solving equation (6) ($\sigma_1 = -5.2, \sigma_2 = 265.2, \sigma_3 = 535.7$ *MPa*). Furthermore, to calculate the Von-Mises effective stress, we should use equation (7) [40]:

$$\overline{\sigma} = \sqrt{0.5}\left(\left[(\sigma_2 - \sigma_3)^2 + (\sigma_3 - \sigma_1)^2 + (\sigma_1 - \sigma_2)^2\right]\right)^{0.5} = 468.43\ MPa \tag{7}$$

As seen the above-mentioned computations are in agreement with the Von-Mises provided by ANSYS (Fig. 3) and fall in the range shown in the colored legend in Fig. 3. It is noteworthy to mention that, roll bonding is a non-homogenous process in that stress/strain values could have fluctuated during the process and therefore it is logical to assume that different amount of stress for a given time can

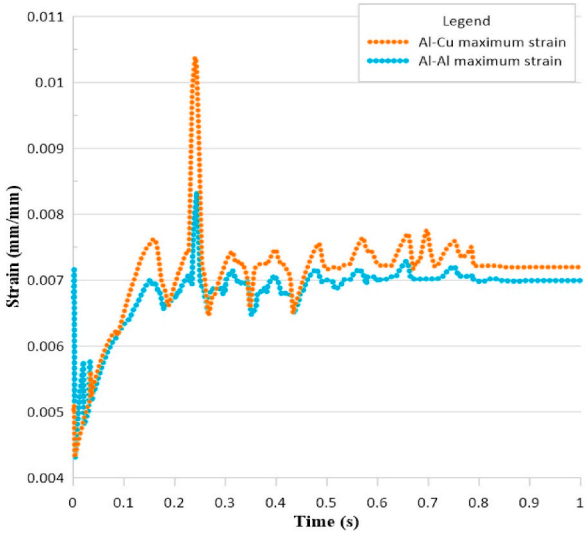

Fig. 5. Equivalent strain distribution for Al-Al and Al–Cu upon simulation.

be obtained during rolling.

Also, it should be noted that effective strain can be calculated similar to effective stress as stated above using equations (8) and (9) [40]:

$$\varepsilon_{ij} = \begin{pmatrix} \varepsilon_{xx} & \varepsilon_{yx} & \varepsilon_{zx} \\ \varepsilon_{xy} & \varepsilon_{yy} & \varepsilon_{zy} \\ \varepsilon_{xz} & \varepsilon_{yz} & \varepsilon_{zz} \end{pmatrix} \tag{8}$$

And for effective strain:

$$\overline{\varepsilon} = \sqrt{(2/3)(\varepsilon_1^2 + \varepsilon_2^2 + \varepsilon_3^2)} \tag{9}$$

where ε_{ij} is the strain tensor and $\varepsilon_{1\text{-}3}$ are principal strains. Also, a summary of the equivalent strain calculated by simulation is shown in Fig. 5. As seen, no markable changes in strain for Al–Al and Al–Cu have occurred, this is because both materials experienced a similar level of reduction in thickness regardless of the type of initial metals.

In order to have an in-depth analysis of the data obtained from this simulation, 3-dimensional graphs of different stresses for Al–Al and Al–Cu composite were drawn as seen in Fig. 6 (a) to (d). As seen, for Al–Al bimetal, the maximum peaks of the diagrams reached in a lower value of Von-Mises stress as compared to that of Al–Cu. This confirms that the joining of Al–Al metal merits lower values of rollers force as also stated in earlier paragraphs. However, for Al–Cu, the principal stress should be higher enough for joints to be bonded. This finding is in agreement with the authors' previous investigations related to Al-Cu [9,33] and testifies to the fact that dissimilar metals need further deformation to initiate bonding. It is also noteworthy that the greater work hardening of the Cu side, due to lower SFE as stated above, is an important metallurgical aspect that could have possibly increased the stress levels during the rolling process of Al-Cu.

For maximum shear stress, on the other hand, the origin of the shear stress should be related to the friction between the roller's surface and metal [5]. As both the surfaces were smooth and the friction coefficient is negligible i.e., 0.1, the shear stress is way lower than the Von-Mises and principal stresses (Fig. 6 (b) and (d)).

For the peeling test, moreover, a simulation is proposed and the results of the test are shown in Fig. 7 (a) and (b). As seen, during the peeling test two surfaces de-bonds as a result of the formation of cracks that are nucleated at the interface of the Al–Cu joints as also confirmed elsewhere [33]. De-bonding of the layers was concentrated at the interface of the metals, as the peeling test continued, cracks propagated on the interface of the Al–Cu. To evaluate the strength of the bonding, the output of the ANSYS software is plotted as shown in Fig. 8. As it can be seen, the bonding of the layers was strong, and equivalent stress reached its highest point during the test.

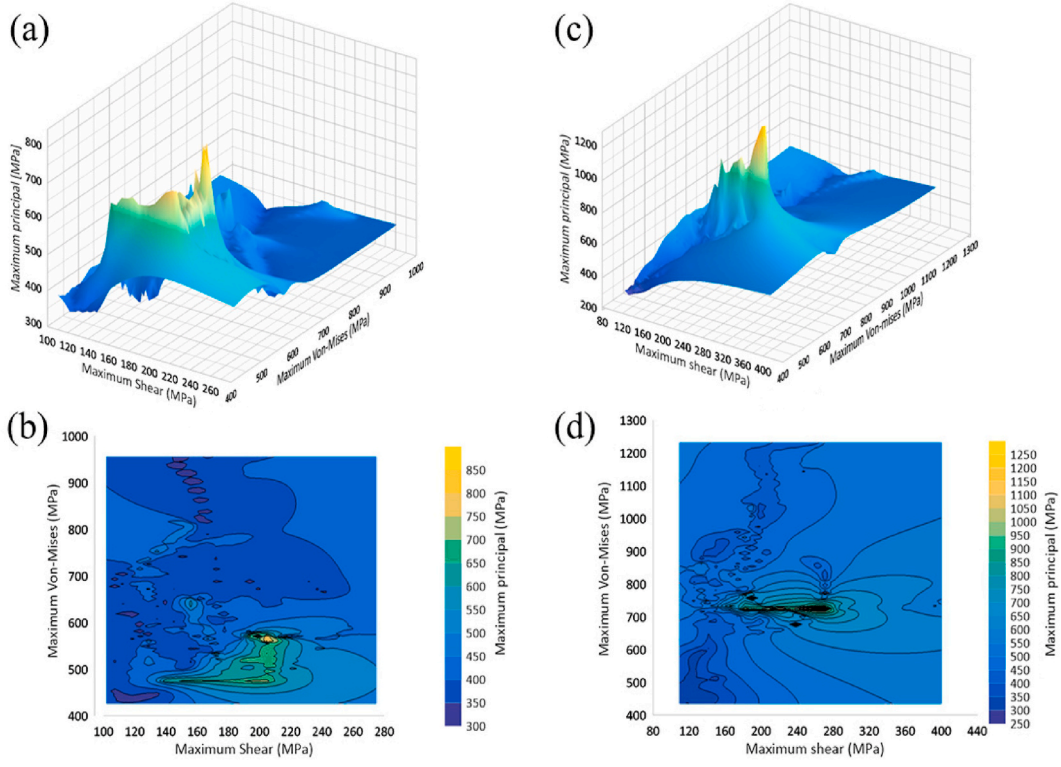

Fig. 6. A 3D diagram of principal-shear-Von Mises stresses showing maximum and minimum values for a, b) Al–Al, and c, d) Al–Cu bimetals.

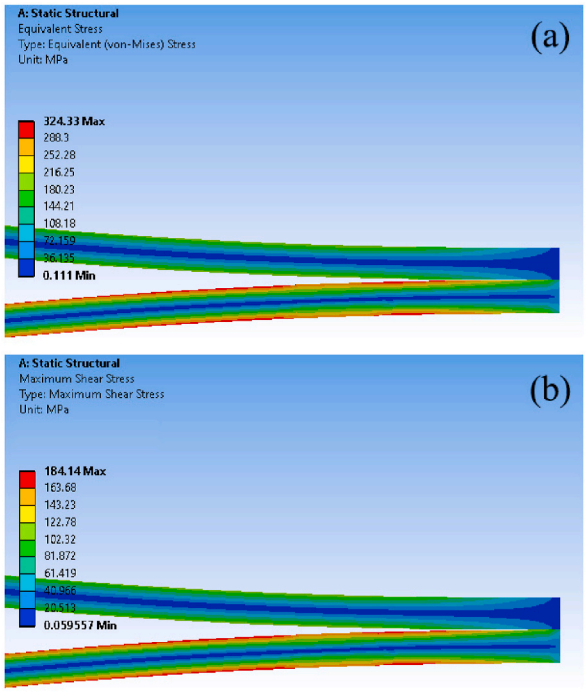

Fig. 7. 2D simulation of the peeling test, a) Von-Mises stress, and b) maximum shear stress.

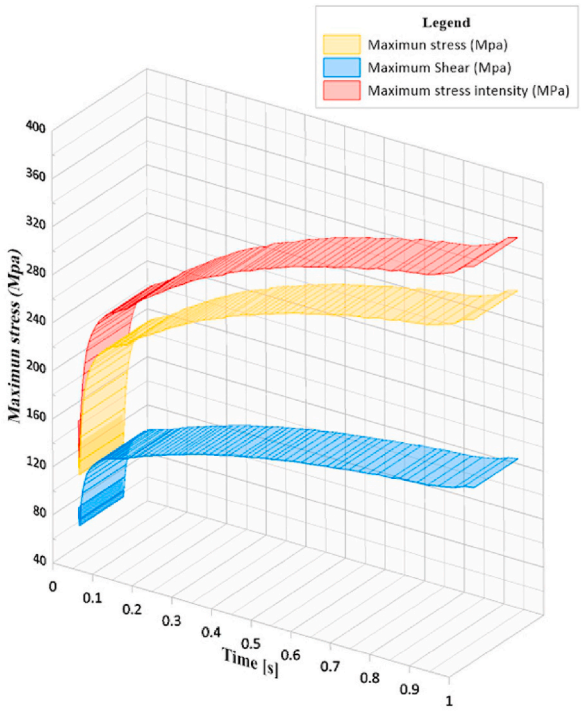

Fig. 8. Stresses-time diagram obtained from ANSYS following simulation of peeling test.

For the shear stress, however, the results show a lower value for the materials as the cracks grow during the test. This could be due to the localized bonding. In fact, during the rolling process, some cracks form at the interface of the Al–Cu, and bonding occurs where fresh metal beneath these cracks is extruded and meets the adjacent cracks (this is discussed in detail later). The initial lower values for all stresses at the beginning may be because a high level of force was needed for the crack to nucleate and after that, the force was

stabilized and reached a certain level because a great population of the cracks formed along the interface, and as the first crack nucleated, a constant force was needed for their further growth. Similar experimental results were observed in our previous work conducted on the Al–Cu CRBed material [33], which is in good agreement with the present simulations.

For qualitative investigation of the proposed simulation and to support the abovementioned discussions, the surface of the Al and Cu layers, after the peeling test, were investigated using microscopy techniques. As seen in Fig. 9 (a) and (b), a great population of microcracks formed during the rolling process as pointed out by arrows. For both layers, it is obvious that the cracks formed and propagated during the peeling process. Based on similar observations by our research study [9], it is claimed that during the cold rolling, a great number of cracks nucleated at the interface of the sheets, and fresh underlying metals extruded along these localized cracks. As the two metals meet at the interface, bonding is established as a result of the rolling pressure. But no bonding would be expected at non-bonded regions. Indeed, in these areas, no cracks were formed and in turn, no bonding could be initiated. During the peeling test, however, the material departed as the crack propagated through both bonded and non-bonded interfaces. Also, for calculating the strength of the bonding of two layers, equation (10) can be used [9]:

$$\text{Peel strength} = \frac{Average\ load\ (N)}{Bond\ width\ (mm)} \tag{10}$$

3.2. Crack behavior simulation

The Al–Cu composite is subjected to deformation after cold rolling by a simulation technique. In this regard, the behavior of an arbitrary crack for the Al and Cu layers was simulated separately without considering the effect of the interface. This is due to the fact that the interface of the joints plays a role in the fracture mechanism and its complicated role in changing the mode of the fracture is not the subject of the present study. Thus, the authors decided to evaluate the layers separately. At first, a hypothetical V-shape crack was defined and the deformation was applied. As it is obvious from the contours in Fig. 10 (a) and (b), the metals' response to the deformation varied as the crack grew larger. The amount of plastic deformation around the crack tip is different for Al and Cu. For the Al layer, Fig. 10 (a), a large area of metal was involved in plastic deformation i.e., a larger affected zone. However, for the Cu layer, the amount of deformation was limited to a small area in front of the crack as compared to the Al layer. It confirms that the crack formation during the test can easily propagate through the softer metal i.e., Al. Also, it can be concluded that during the deformation, the Cu layer, may resist crack propagation as compared to the other layer. Therefore, during crack growth, the plastic deformation area was smaller for the Cu layer and the crack required more deformation for growth. Therefore, for the metals with lower SFE, such as Cu in this study, crack propagation is way more difficult. For the Al layer, in contrast, the area of plastic deformation was high and the ability of the crack to grow larger was enhanced as compared to that of the Cu layer as confirmed by the stress distribution in Fig. 10 (b). However, the plastic deformation in front of both metals has some similarities. It is known that both metals have a similar crystal structure (face-centered cubic) and the plastic deformation in front of the cracks was almost similar in that the Al shows more plastic deformation as compared to that of Cu.

In addition, as stated above, Cu requires more plastic deformation for crack propagation as a result K_I would be expected to increase for the Cu side. For a precise quantitative investigation of the stress intensity factor in this study, K_I needs to be evaluated for the composite.

Based on Liu et al. [41], the K_I at the tip of the V notch crack is calculated using equations (11)–(13):

$$\sigma = \frac{K_I}{\sqrt{2\pi x}} \text{ for } x > 0 \tag{11}$$

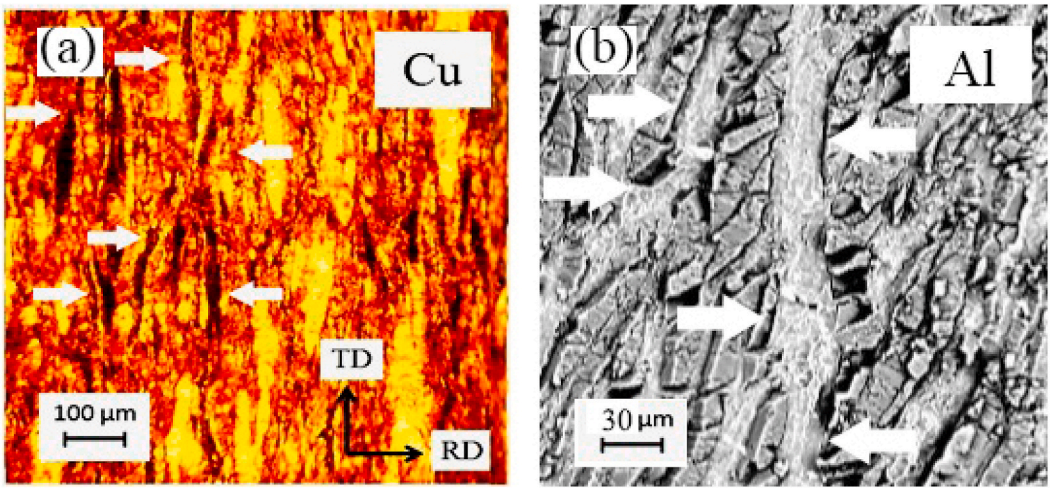

Fig. 9. Fracture surfaces after peeling test: a) Cu surface (OM) and b) Al surface (SEM) [Note that some cracks are pointed by arrows].

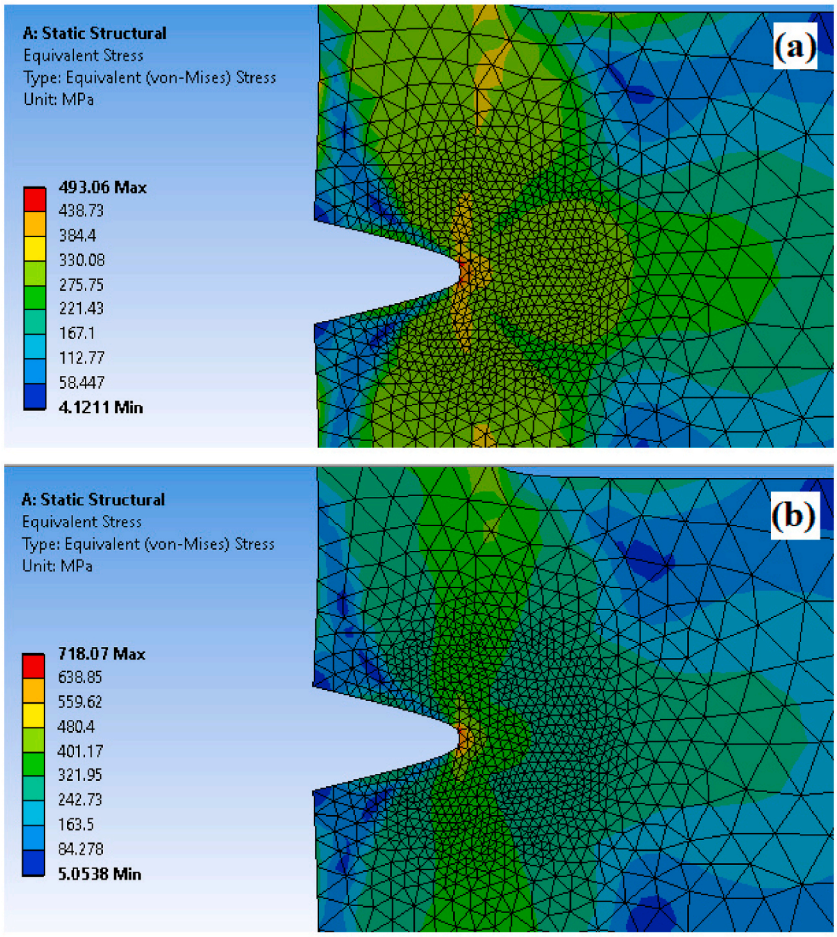

Fig. 10. Equivalent Von-Mises stress distribution at the crack tip during the deformation for: a) Al, and b), Cu layers.

$$K_I = \sigma\sqrt{\pi a}\,.\; f(\mu) \tag{12}$$

And for f (μ) we have:

$$f(\mu) = \left(1.12 - 0.23\left(\frac{a}{w}\right) + 10.56\left(\frac{a}{w}\right)^2 - 21.74\left(\frac{a}{w}\right)^3 + 30.42\left(\frac{a}{w}\right)^4\right) \tag{13}$$

The maximum stress intensity factor (K_I) for Al and Cu was evaluated by FEM to be about 237 and 353 MPa $mm^{0.5}$, respectively (Fig. 11) and from equations above (considering a = 5 mm, σ is the difference of maximum and minimum normal stress, max = 321.6 and min = 307.3 MPa for Al and max = 399, and min = 303 MPa for Cu side, and f (μ) = 1.1), K_I for Al and Cu can be measured as 62 and 418.5 Mpa.$mm^{0.5}$, respectively. As seen, the calculations of K_I are appropriate for predicting Cu rather than Al. The reason for this controversy is not clear, however, some factors such as the effect of the interface, grain size, texture, and grain boundaries that are absent in the FEM model can be reasons for the differences in calculated K_I. The interface that is excluded in this research may lead to a complex form of stress intensity factor such as initiating K_{II}. Therefore, this area of our study is obscure and needs further investigation. It is also proposed that the maximum tension at the tip of the crack can be obtained using equation (14) for semi-finite plates [41]:

$$\sigma_{max} = \frac{(a+\rho)}{\sqrt{\rho^2 + 2a\rho}}\;.\;3.36\sigma \tag{14}$$

For a comparison between data given from simulations; maximum shear, Von-Mises, and normal stresses in front of the crack were calculated and plotted in Fig. 12. It is shown that by increasing the time of the simulations, the stresses increased followed by a steady-state behavior. This could be related to the increasing work hardening and non-linear behavior of the metals during plastic deformation. As it can be concluded from this figure, the simulation can predict the material's behavior aligned with the analytical calculations above. It is worth noting that the maximum stress in front of the crack tip is higher for Cu layers. Once again, the results should be related to greater work hardening and dislocations accumulation in the vicinity of nucleated cracks for the Cu side, and thus

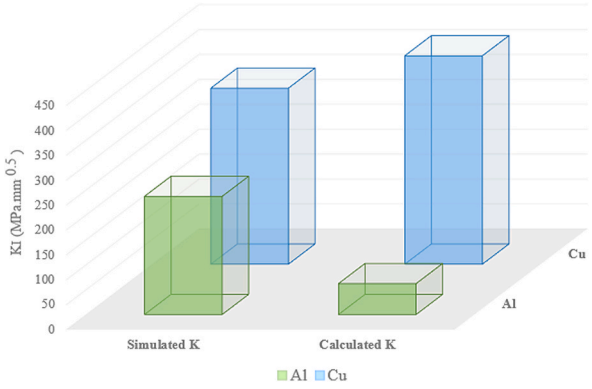

Fig. 11. Stress intensity factor (K_I) variations for simulation and analytical calculations in Al and Cu.

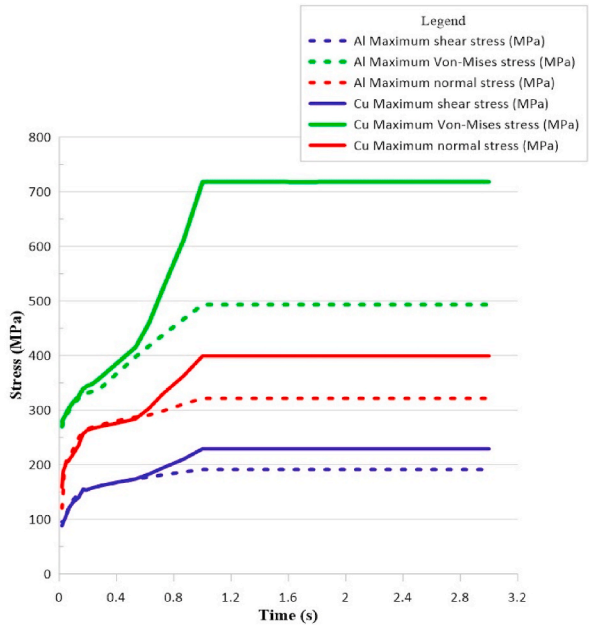

Fig. 12. Diagrams obtained from ANSYS for the relevant stresses in Al and Cu for comparison.

the growth of the crack needs further deformation. This finding also is consistent with earlier discussions and confirming the previous investigations.

To evaluate the nature of the fracture during the test, SEM fractography is conducted as seen in Fig. 13. It can be concluded from this figure that as the crack propagated, a lamellar-shaped structure also known as "cup and cone" can be formed. This observation is a result of ductile fracture. It is necessary to add that during the test, layers fractured and departed as the crack grew larger. In this stage, a mixed fracture mode may have determined the fracture behavior and the deviation of the stress intensity factor in our calculation should have lied in this phenomenon. As the crack propagates through the layers, it finally reaches a critical size, and the rupture has occurred from the base composite during the test.

4. Conclusion

An Al–Cu composite was successfully produced, characterized, and its behavior simulated using the finite element method, and the results obtained from the study are summarized below.

- A deviation at the end part of the simulated sample was observed when dissimilar Al–Cu metallic sheets were CRBed. By replacing it with a similar metal-metal, the deviation was diminished.
- Stress analysis of the CRB process revealed that for Al–Cu a larger value of Von-Mises stresswas required to initiate bonding.

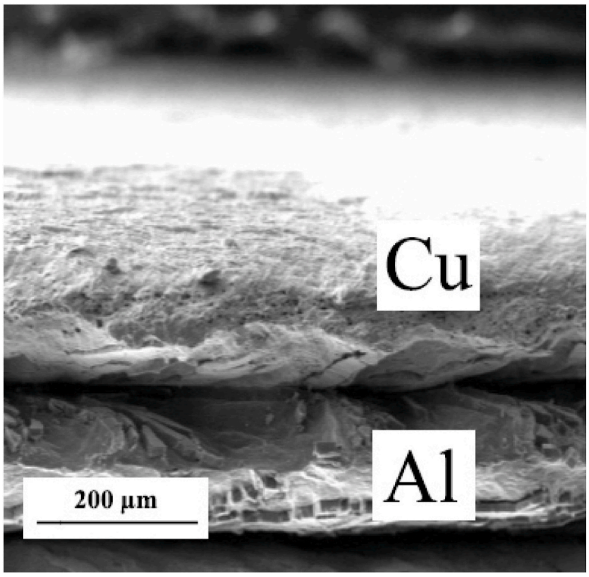

Fig. 13. SEM image for fractography of the Al–Cu after the rupture.

- During the CRB process and peeling test, cracks were initiated at the interface of the material and propagated through the Al–Cu joint to depart the layers.
- The fracture surface of the peeled Al–Cu declared a great population of microcracks that formed during the rolling process.
- At the crack tip, a plastic deformation zone was created with larger values for Cu as compared to Al.
- Mode I fracture was the main phenomenon for the destruction of the Al–Cu for both the peeled and V-notched samples.

Additional information

No additional information is available for this paper.

CRediT authorship contribution statement

Vahid Yousefi Mehr: Writing – review & editing, Writing – original draft, Investigation, Formal analysis, Data curation. **Mohammad Reza Toroghinejad:** Writing – review & editing, Supervision, Investigation, Conceptualization.

Declaration of competing interest

The authors declare that they have no known competing financial interests or personal relationships that could have appeared to influence the work reported in this paper.

References

[1] R. Xu, N. Liang, L. Zhuang, D. Wei, Y. Zhao, Microstructure and mechanical behaviors of Al/Cu laminated composites fabricated by accumulative roll bonding and intermediate annealing, Mater. Sci. Eng., A 832 (2022) 142510.
[2] A.A. Shayanpoor, H.R. Rezaei Ashtiani, Microstructural and mechanical investigations of powder reinforced interface layer of hot extruded Al/Cu bimetallic composite rods, J. Manuf. Process. 77 (2022) 313–328.
[3] R. Sahay, A.S. Budiman, I. Aziz, E. Navarro, S. Escoubas, T.W. Cornelius, F.E. Gunawan, C. Harito, P.S. Lee, O. Thomas, Crystallographic anisotropy dependence of interfacial sliding phenomenon in a Cu (16)/Nb (16) ARB (accumulated rolling bonding) nanolaminate, Nanomaterials 12 (3) (2022) 308.
[4] Y. Chen, J. Nie, F. Wang, H. Yang, C. Wu, X. Liu, Y. Zhao, Revealing hetero-deformation induced (HDI) stress strengthening effect in laminated Al-(TiB2+TiC)p/6063 composites prepared by accumulative roll bonding, J. Alloys Compd. 815 (2020) 152285.
[5] V. Yousefi Mehr, M.R. Toroghinejad, On the texture evolution of aluminum-based composites manufactured by ARB process: a review, J. Mater. Res. Technol. 21 (2022) 1095–1109.
[6] E. Tolouei, M.R. Toroghinejad, V. Yousefi Mehr, H. Monajati, A combination of aluminium strip and brass mesh to process a refined structure composite via accumulative roll bonding: a characterization study, Mater. Char. 205 (2023) 113360.
[7] B.C. Kandpal, J. Kumar, H. Singh, Manufacturing and technological challenges in Stir casting of metal matrix composites–A Review, Mater. Today: Proc. 5 (1) (2018) 5–10.
[8] V. Yousefi Mehr, M.R. Toroghinejad, A. Rezaeian, H. Asgari, J.A. Szpunar, Abnormal texture evolution of accumulative roll bonded Al-Cu by adding alumina particles, Heliyon (2022) e08723.
[9] V. Yousefi Mehr, A. Rezaeian, M.R. Toroghinejad, Effects of processing parameters on the fracture behaviour of cold roll bonded and accumulative roll bonded Al–Cu lamellar composites, Mater. Sci. Technol. 37 (13) (2021) 1096–1106.
[10] H. Lin, Y. Tian, S. Sun, Z. Zhang, Microstructural evolution and mechanical properties of laminated CuAl composites processed by accumulative roll-bonding and annealing, Acta Metall. Sin. (2021) 1–7.

[11] G. Pereira, E. Da Silva, G. Requena, J. Avila, J. Tarpani, Microstructural, mechanical, and fracture characterization of metal matrix composite manufactured by accumulative roll bonding, J. Mater. Eng. Perform. 30 (4) (2021) 2645–2660.
[12] D. Rahmatabadi, M. Pahlavani, M.D. Gholami, J. Marzbanrad, R. Hashemi, Production of Al/Mg-Li composite by the accumulative roll bonding process, J. Mater. Res. Technol. 9 (4) (2020) 7880–7886.
[13] D.C.C. Magalhães, V.L. Sordi, A.M. Kliauga, Microstructure evolution of multilayered composite sheets of AA1050/AA7050 Al alloys produced by Asymmetric Accumulative Roll-Bonding, Mater. Char. 162 (2020) 110226.
[14] P. Kumar, A. Madhup, P.R. Kalvala, S. Suwas, Texture evaluation in AZ31/AZ31 multilayer and AZ31/AA5068 laminar composite during accumulative roll bonding, Defence Technology 16 (3) (2020) 514–519.
[15] A.I. Khdair, A. Fathy, Enhanced strength and ductility of Al-SiC nanocomposites synthesized by accumulative roll bonding, J. Mater. Res. Technol. 9 (1) (2020) 478–489.
[16] B. Rahnama Falavarjani, M.R. Toroghinejad, V. Yousefi Mehr, A novel Cu-carbon nanotube sheet composite manufactured via the ARB process: a microstructural and mechanical study, J. Mater. Res. Technol. 23 (2023) 6054–6064.
[17] M. Samadzadeh, M.R. Toroghinejad, V. Yousefi Mehr, H. Asgari, J.A. Szpunar, Mechanical, microstructural, and textural evaluation of aluminum-MWCNT composites manufactured via accumulative roll bonding at ambient condition, Mater. Chem. Phys. (2024) 128891.
[18] Y. Chen, N. Li, R. Hoagland, X.-Y. Liu, J. Baldwin, I. Beyerlein, J.Y. Cheng, N. Mara, Effects of three-dimensional Cu/Nb interfaces on strengthening and shear banding in nanoscale metallic multilayers, Acta Mater. 199 (2020) 593–601.
[19] C. Ding, J. Xu, X. Li, D. Shan, B. Guo, T.G. Langdon, Microstructural evolution and mechanical behavior of Cu/Nb multilayer composites processed by accumulative roll bonding, Adv. Eng. Mater. 22 (1) (2020) 1900702.
[20] C.-C. Hsieh, M.-C. Chen, W. Wu, Mechanical property and fracture behavior of Al/Mg composite produced by accumulative roll bonding technique, Journal of Composites 2013 (2013).
[21] S. Jiang, R.L. Peng, Z. Hegedűs, T. Gnäupel-Herold, J. Moverare, U. Lienert, F. Fang, X. Zhao, L. Zuo, N. Jia, Micromechanical behavior of multilayered Ti/Nb composites processed by accumulative roll bonding: an in-situ synchrotron X-ray diffraction investigation, Acta Mater. 205 (2021) 116546.
[22] E. Mostafazadeh, H. Jafarzadeh, Fabrication of Al/Cu composite reinforced with AISI 304 stainless steel wires through accumulative roll bonding and evaluation of their mechanical properties, Trans. Indian Inst. Met. 74 (3) (2021) 583–591.
[23] N. Ye, X. Ren, J. Liang, Microstructure and mechanical properties of Ni/Ti/Al/Cu composite produced by accumulative roll bonding (ARB) at room temperature, J. Mater. Res. Technol. 9 (3) (2020) 5524–5532.
[24] J. Zhang, H. Ding, M. Cai, N. Zhang, H. Qu, S. Li, H. Hou, P. Cao, Nanostructured NiTi shape memory alloy via Ni/Ti nanolamination, Metall. Mater. Trans. 51 (3) (2020) 1051–1055.
[25] H. Pouraliakbar, G. Khalaj, M.R. Jandaghi, A. Fadaei, M.K. Ghareh-Shiran, S.H. Shim, S.I. Hong, Three-layered SS321/AA1050/AA5083 explosive welds: effect of PWHT on the interface evolution and its mechanical strength, Int. J. Pres. Ves. Pip. 188 (2020) 104216.
[26] M.D. Gholami, R. Hashemi, B. Davoodi, Investigation of microstructure evolution on the fracture toughness behaviour of brass/low carbon steel/brass clad sheets fabricated by cold roll bonding process, J. Mater. Res. Technol. 25 (2023) 2570–2588.
[27] R. Kocich, L. Kunčická, Development of structure and properties in bimetallic Al/Cu sandwich composite during cumulative severe plastic deformation, J. Sandw. Struct. Mater. 23 (8) (2021) 4252–4275.
[28] V. Yousefi Mehr, M.R. Toroghinejad, Microstructural investigation of an Al–Cu lamellar nanocomposite produced by accumulative roll bonding process under the heat treatment condition: an analytical, experimental, and finite element study, J. Mater. Res. Technol. 20 (2022) 1028–1042.
[29] V. Yousefi Mehr, M.R. Toroghinejad, Complementary research on the Al–Cu nanostructured composite processed by ARB: finite element, crystal plasticity, intermetallic, and failure analysis, J. Mater. Res. Technol. 24 (2023) 5934–5946.
[30] D. Rahmatabadi, B. Mohammadi, R. Hashemi, T. Shojaee, An experimental study of fracture toughness for nano/ultrafine grained Al5052/Cu multilayered composite processed by accumulative roll bonding, J. Manuf. Sci. Eng. 140 (10) (2018) 101001.
[31] V. Yousefi Mehr, M.R. Toroghinejad, J. Dutkiewicz, Unveiling slip/nanotwin/nano shear band deformation mechanisms at the copper side in a roll-welded aluminum/copper couple, Mater. Char. 203 (2023) 113039.
[32] M.R. Azad, A. Ghasemi, H. Pouraliakbar, M.R. Jandaghi, On the Al/cu dissimilar joints produced through simple cold compression, Trans. Indian Inst. Met. 68 (2015) 991–998.
[33] V. Yousefi Mehr, M.R. Toroghinejad, A. Rezaeian, The effects of oxide film and annealing treatment on the bond strength of Al–Cu strips in cold roll bonding process, Mater. Des. 53 (2014) 174–181.
[34] J.-y. Sun, H.-q. Zhu, S.-h. Qin, D.-l. Yang, X.-t. He, A review on the research of mechanical problems with different moduli in tension and compression, J. Mech. Sci. Technol. 24 (9) (2010) 1845–1854.
[35] N. Nie, L. Su, G. Deng, H. Li, H. Yu, A.K. Tieu, A review on plastic deformation induced surface/interface roughening of sheet metallic materials, J. Mater. Res. Technol. 15 (2021) 6574–6607.
[36] H. Yu, A.K. Tieu, C. Lu, A. Godbole, An investigation of interface bonding of bimetallic foils by combined accumulative roll bonding and asymmetric rolling techniques, Metall. Mater. Trans. 45 (9) (2014) 4038–4045.
[37] M. Hosseini, N. Pardis, H.D. Manesh, M. Abbasi, D.-I. Kim, Structural characteristics of Cu/Ti bimetal composite produced by accumulative roll-bonding (ARB), Mater. Des. 113 (2017) 128–136.
[38] H. Yu, A.K. Tieu, C. Lu, X. Liu, A. Godbole, H. Li, C. Kong, Q. Qin, A deformation mechanism of hard metal surrounded by soft metal during roll forming, Sci. Rep. 4 (1) (2014) 1–8.
[39] F.J. Humphreys, M. Hatherly, Recrystallization and Related Annealing Phenomena, Elsevier, 2012.
[40] W.F. Hosford, R.M. Caddell, Metal Forming: Mechanics and Metallurgy, Cambridge university press, 2011.
[41] M. Liu, Y. Gan, D.A. Hanaor, B. Liu, C. Chen, An improved semi-analytical solution for stress at round-tip notches, Eng. Fract. Mech. 149 (2015) 134–143.